Acta Scientific COMPUTER SCIENCES

Volume 4 Issue 8 August 2022

Research Article

Multi-input Rectifier Stage for Hybrid Renewable Energy System

M Pandikumar[1], R Sundreswaran[2]* and M Shnamugapriya[2]

[1]Department of Electrical and Electronics Engineering, Sri Sivasubramaniya Nadar College of Engineering, Tamil Nadu, India

[2]Department of Mathematics, Sri Sivasubramaniya Nadar College of Engineering, Tamil Nadu, India

***Corresponding Author:** R Sundreswaran, Department of Mathematics, Sri Sivasubramaniya Nadar College of Engineering, Tamil Nadu, India.

Received: May 14, 2022

Published: July 18, 2022

Abstract

Concern over the state that our planet is in as it continues to deteriorate is causing environmentally friendly solutions to become more popular than ever. Because of environmental concerns, green solutions are becoming increasingly popular. In this paper, a redesigned rectifier stage is applied to an example of a hybrid energy system. The load can be supplied by either of the two sources, based on how readily it can be met by the various sources of energy, in this configuration. In order to get rid of higher order harmonics, this fused converter with a Cuk-SEPIC, does not require any additional input filters to be installed. The presence of the harmonics has a negative impact on the generator's lifespan, heating issues, and overall performance.. Due to its fused rectifier with multiple inputs, the maximum power point tracking (MPPT) can be utilised whenever wind and sunlight are available to generate electricity. When it comes to wind and PV, we'll use an adaptive MPPT algorithm and a common perturb and observe procedure. The proposed system's operational analysis will be discussed in this paper. For the sake of emphasising the advantages of the circuit under consideration, simulation results are presented. When one energy source isn't able to keep up with the demand, another can step in to fill the gap. MPPT control has been proposed for a number of hybrid wind/PV systems, and in addition to that, the utilisation of rectifiers and inverters has been debated.

Keywords: Wind Energy; Solar Photovoltaics; SEPIC Converter; Cuk Converter; Hybrid Systems

Introduction

Fossil fuels are being eschewed by an increasing number of people concerned about warming of the planet's atmosphere and diminishing supplies of fossil fuels as fuel sources. Climate change and the depletion of fossil fuels necessitate a new approach. Fossil fuels are a major source of concern for many people. The greatest potential for satisfying our energy requirements lies not only in hydropower, but also in wind and photovoltaic energy. Wind and photovoltaic energy, rather than hydropower, have the greatest possible significance to fulfil our needs in terms of energy. Unreliability is inherent in wind and photovoltaic power generation due to the intermittent nature of these sources of energy. The most common disadvantage associated with wind and solar power systems is that they produce intermittent amounts of energy. Wind power, on the other hand, has the ability to generate significant amounts of electricity, despite the fact that its availability is highly unpredictable. It's similar to the sun, which emits energy all day long, but its intensity fluctuates due to clouds, birds, and other objects casting shadows.

The other energy source can make up for the shortfall caused by the absence of one of the sources or by the source's inability to

adequately meet the load demands. Because of this, the overall efficiency and the dependability of the system has room for improvements, that can be made by merging and installing these two intermittent power sources with the maximum power point tracking (MPPT) algorithms. It has been suggested to use MPPT to control hybrid wind/photovoltaic power systems, and the topic is currently being discussed. Harmonics of high-frequency current are put into wind turbine generators, and to get rid of them. The methods that are described in the appropriate literature require the application of the passive input filters. As can be seen in figure 1, the rectifier stage in regard to every source of power generated by renewable energy consists of a parallel connection of one DC/DC boost converter, which is common in published systems. Combining the sources coming from the DC end while preserving a relatively uncomplicated multi-input structure is one way to accomplish MPPT for each individual renewable energy source. The buck and buck-boost converters are combined in this design.

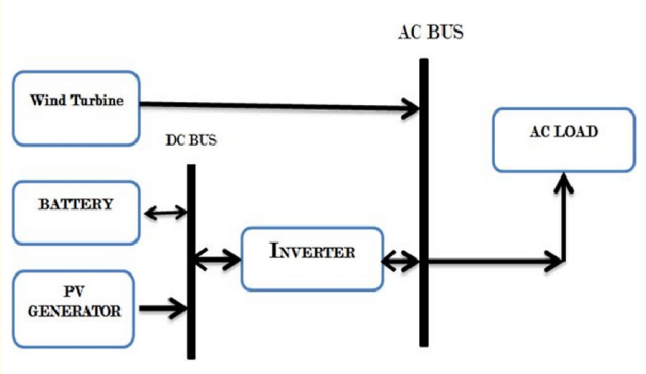

Figure 1: Hybrid system featuring multiple boost converter connections.

Because harmonics are present in the current that is flowing through the generator, the lifespan of the generator is reduced, and the quantity of power that is disposed of as a result of heating is increased. This project proposes an alternative structure for the multi-input rectifier that is typically utilised in hybrid power generation systems that make use of both solar and wind power. The Cuk and SEPIC converters have been combined into a single device in the new design.

The proposed topology has the following parts:

- Separate PFC Input Filters are not required because of the built-in nature of these two converters.
- Each renewable source can be used for step up/down operations (has the capability to accommodate a wide range of PV and wind inputs).
- Each source can benefit from MPPT.
- There's support for both individual and simultaneous use.

Increasingly more people are opting to buy hybrid electric vehicles (HEVs) and electric vehicles (EVs) as a response to the rising cost of oil and growing concerns about the environment, as described by Rahman, K. M., Patel, N. R., Ward, T. G., Nagashima, J. M., Caricchi, F., and Crescimbini, F. (2006) in their paper, "Application of direct-drive wheel motor for fuel cell electric and hybrid electric vehicle propulsion system" [1].

This avoids the need for an electronic brake resistor because of the motor's ability to dissipate the braking power. If the controller is set to maximise the stator voltage or current, the losses in the motor will increase as a result. About the DC-link capacitor, field weakening, flux braking, and overvoltage are discussed by M. Hinkkanen and J. Luomi [2].

C. H. Rivetta, A. Emadi, G. A. Williamson, R. Jayabalan, and B. Fahimi discussed the behaviour of the converter system using phase plane analysis on buck and boost dc-dc converters with CPLs and a state feedback controller, as well as constant power loads, control, and dc-dc converters [3].

The operating principles made by the capacitor voltage synthesis multilevel converters are based on the features, constraints, and application areas for the multilevel converters. J. S. Lai, J. Rodriguez, J. Lai, and F. Peng examine the most critical topologies, such as diode-clamped inverters (neutral-point clamped), capacitor-clamped inverters (flying capacitors), and multilevel inverters [4,5].

For large electric drives, a multilevel cascade inverter with separate dc sources and a multilevel diode-clamped back-to-back converter has been proposed. This converter has low output voltage THD and high efficiency, and power factor has been discussed by L. M. Tolbert, F. Z. Peng, and T. G. Habetler [6-8].

It was discussed by M. Shen and his colleagues that there are two distinct approaches to controlling the constant boost on the Z-source inverter, both of which aim to minimise voltage stress while simultaneously achieving maximum voltage gain at any modulation index. These methods are able to do this because low-frequency ripple that is not in relation to the frequency of the output does not occur, were proposed [9-12].

A cascaded H-bridge multilevel boost inverter for EVs and HEVs without inductor is proposed in this paper. Typically, each H-bridge requires a DC power supply. A capacitor serves as the DC power source for a standard three-leg inverter (one leg for each phase). The H-bridge is connected in series with each leg. In this system, the use of large inductors is completely eliminated, which decreases the cost and space of the system. The desire to reduce the vehicle emission and improvement in fuel economy can be achieved.

Modelling of the wind turbine system

A wide range of wind system perturbations can be accurately predicted using the various component models presented here.

Power available from the wind turbine

The amount of power that can be generated by winds currently available, power distribution across the machine's curve, and the efficiency with which a wind turbine can generate power from changing winds is dependent on a number of factors, including the device's capacity to adapt to shifting wind speeds and directions, as well as other aspects of the environment. As a result of wind turbines, mechanical power can be generated as follows [9]:

$$P_{Am} = 0.5\rho C_p A U_W^3 \ (\text{watts}) \text{ -------- (1)}$$

Analytically, a third-degree polynomial can be used to calculate the power coefficient of any wind turbine, as shown in the example below.

$$C_P = \frac{16}{17}\frac{\lambda}{\lambda + \frac{1.32 + \left[\frac{\lambda - 8}{20}\right]^2}{B}} - 0.57\frac{\lambda^2}{\frac{L}{D}\left(\lambda + \frac{1}{2B}\right)} \text{ ---------- (2)}$$

Where is the ratio of tip to blade speed

Defined as: $\lambda = \frac{rw_A}{U_W}$

The lift-to-drag ratio (L/D) is represented by the number of blades in the wind turbine (B) in the formula above. It is known that B and L/D can be calculated from the technical characteristics of the wind turbine Equation (2), which is valid from 4 to 20 for B=1, 2 or 3, and from L-D.≤25 with a high degree of accuracy.

Any WT with variable speed that also has the ability to adjust the effective rotational aerodynamic efficiency can simply be taken into account using an appropriate expression for the pitch angle-dependent constant C_P.

The mechanical part of the wind turbine model consists of the following parameters [9]: turbine blade speed (ω_B), the hub speed (ω_H), the gearbox speed (ω_G) and the generator's mechanical speed (ω_M). The relationship between the generator's mechanical speed (ω_M) and its electrical (ω_A) angular velocities can be expressed as . Despite the fact that the angular velocities on both sides of the gearbox are $\omega_M=R_G\omega_G$ where P is the number of poles and is the transmission ratio. There is a correlation between angular velocities and shaft angles and is given by . It is possible to standardize Equation (3) based on the three-phase volt-ampere rating of the generator.

$$J_B\frac{d\omega_B}{dt} = T_{Am} - D_B\omega_B - D_{BH.}(\omega_B - \omega_H) - K_{BH.}(\theta_B - \theta_H)$$

$$J_H\frac{d\omega_H}{dt} = -D_H\omega_H - D_{BH.}(\omega_H - \omega_B) - D_{HG}(\omega_H - \omega_G) - K_{HB.}(\theta_H - \theta_B) - K_{HG}(\theta_H - \theta_G)$$

$$J_G\frac{d\omega_m}{dt} = -T_{A_e} - D_G\omega_m - \frac{D_{HG}}{R_G}(\omega_G - \omega_H) - \frac{K_{HG}}{R_G}(\theta_G - \theta_H)$$

----------(3)

Using the above model, one can study how a machine behaves in high-turbulence conditions like gusts of wind. On the other hand, mechanical dynamics are frequently ignored, which is especially common in machines that have a great deal of inertia or when there is a lack of availability of the necessary parameters. Using the above model, one can study how a machine behaves in high-turbulence conditions like gusts of wind. However, mechanical dynamics are often overlooked, especially in machines with a lot of inertia or when there is a lack of availability for the necessary parameters. As a result, the third equation can be simplified to a single differential equation if the dynamics of the hub are disregarded and only the shaft is thought of as being rigid.

$$\omega_B = \omega_m = \frac{2}{P}\,\omega_A.$$

$$\frac{d\omega_A}{dt} = \frac{\omega_o}{2H_A}\left(T_{Am} - T_{Ae} - \frac{D_A}{\omega_o}\omega_A\right) \text{ ---------(4)}$$

In contrast to the other quantities, which are expressed using the per-unit system, The swing equation, which is denoted by the equation 4, is derived from the kVA rating of the machine, which deals with rotational velocity.

Asynchronous generator model

According to popular belief, an asynchronous generator is installed on the WT. Simplified Park equations serve as the basis for the asynchronous machine equations. The stator electrical transients are ignored in comparison to the rotor ones, which is the most important. The synchronous reference frame is taken into account in the per-unit (p.u.) system of these equations. Asynchronous motors are the technical term for wind turbine generators used in the generation of electric power (negative loads). The asynchronous machine's torque and slip can tell you if it's a generator or a motor [13-20]. These equations are based on algebraic stator theory:

$$V_d = E'_d + r_s I_d - X' I_q$$

$$V_q = E'_d + r_s I_q + X' I_d \text{ ----------(5)}$$

Rotor winding dynamics are depicted in these differential equations as follows.

$$\frac{dE'_d}{dt} = T'_o\left[-E'_d - (X - X')I_q + s\omega E'_d\right] \text{ ---------- (6)}$$

$$\frac{dE'_q}{dt} = T'_o\left[-E'_q + (X - X')I_d - s\omega E'_d\right] \text{ ----------(7)}$$

The equation for the electromagnetic torque is as follows:

$$T_{Ae} = E'_d I_d + E'_q I_q \text{ ---------- (8)}$$

Power, both active and reactive, as well as voltage and current, can be calculated using the following relationships:

$$P_{Ae} = Re\{V_t I_A^*\} \text{ ----------(9)}$$

$$Q_{Ae} = Im\{V_t I_A^*\} \text{ ----------(10)}$$

$$V_t = \sqrt{(V_d^2 + V_q^2)} \text{ ---------(11)}$$

$$I_t = \sqrt{(I_d^2 + I_q^2)} \text{ ----------(12)}$$

The number of differential equations in a wind park with a large number of units increases significantly. As a result, a number of wind turbines can be assumed to operate in the same set of wind circumstances. Groups of n identical machines in the wind park can be replaced with one identical machine for each group. Machines of the same make and model should be placed in the same group. A machine that replaces n identical machines is given its parameters by the following equations:

$$H_{An} = nH_A,\ T'_{on} = T'_n,\ r_{sn} = \frac{r_s}{n},,$$

$$X_n = \frac{x}{n},\ X'_n = \frac{x'}{n} \text{ ---------(13)}$$

As a result, a variable-speed mode for wind turbines that use power electronics to simulate the control of their electrical connection to the grid.

Sepic converter

As depicted in figure 2, a single-ended primary-inductor converter (SEPIC) is a DC-DC converter in which the output voltage can be set to be greater, lower, or the same as the input voltage. The duty cycle of the SEPIC's control transistor determines how much current flows through the device's output.

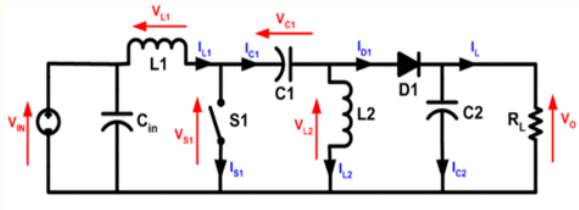

Figure 2: SEPIC converter schematic diagram.

It is a type of converter that is comparable to a conventional buck-boost converter; however, it possesses advantages such as output that is not inverted (the output voltage is the same polarity as the input voltage) and a partitioning off of the input and the output (provided by a capacitor in series).

Continuous mode

For a SEPIC, "continuous mode" means that the current flowing through inductor L_1 never drops below zero. During steady-state operation, the voltage that is input (V_{in}) is equal to the average voltage that is measured across capacitor C_1 (V_{C1}). There is no other source of current for the load besides inductor L_2, because capacitor C_1 blocks direct current (DC). To put it another way, regardless of the input voltage, Inductor L_2 (I_{L2}) has an average current flow equal to the average load.

Discontinuous mode

A SEPIC has entered a mode of conduct that is considered discontinuous as long as the current that is flowing through the inductor L_1 does not reach zero.(also known as a discontinuous mode).

Reliability and efficiency

The drop in voltage and duration of the diode's switching D1 are two crucial factors that determine the dependability and effectiveness of the SEPIC. The switching time of the diode needs to be extremely fast in order to prevent components from being damaged as a result of high voltage spikes that occur across the inductors. It is possible to use either Schottky or regular diodes.

The resistances of the converter's inductors and capacitors can also have an effect on the efficiency and ripple of the device. Less energy is lost as heat when inductors have lower series resistance, resulting in higher efficiency (the load is receiving a larger proportion of the input power). Even in C_1 and C_2, where the current frequently reverses direction, capacitors characterized by a reduced equivalent series resistance (ESR) should be utilised so that ripple is reduced and heat is not allowed to accumulate. This is necessary in order to avoid damaging the circuit.

Rectifier stage with multiple inputs

Figure 3 depicts a hybrid energy system's proposed rectifier stage, where one input is connected to the PV array's output and One of the generator's outputs is connected to another input. Both the SEPIC converter and the Cuk output inductor belong to the same system which makes the converters to operate as one. In the event that information from a single source cannot be obtained, each converter can continue to function independently. The situation where only wind is available. A SEPIC converter is formed when D1 is turned off and D2 is turned on; changes have been made to the proposed circuit's input-to-output voltage relation and is given by equation (14). However, in the event that only the PV source is accessible, D2 will be shut down, while D1 will continue to operate normally throughout the entire process, transforming the circuit into a Ku converter. The connection that exists between the voltage that is present at the input and the voltage that is present at the output is given by equation (15). Both converters have the ability to perform buck/boost conversion, which enables the system to have greater design flexibility, if maximum power point tracking (MPPT) control is performed using duty ratio control.

$$\frac{v_{dc}}{v_w} = \frac{d_2}{1-d_2} \qquad \text{----------(14)}$$

$$\frac{v_{dc}}{v_p} = \frac{d_1}{1-d_1} \qquad \text{----------(15)}$$

It's possible that the states I, II, and IV will be switched if M1's turn-on time is longer than that of M2. Similarly, if the conduction periods of the switch were to be switched around, the transitioning states are going to be I, III, and IV. Figure 1 shows the inductor current waveforms for each possible state of switching in the case of switching states I through IV, assuming that d_2 is greater than d_1. PV is the average input current; I_i, W is the rectifier's input current measured by its RMS value (wind gust); and I_{dc} is the average amount of current that is generated by the system. As can be seen in figure 4, the main waveforms used to illustrate the various states of the system under test are shown. There will be an explanation of the mathematical formula for the total output and input voltage in the following section.

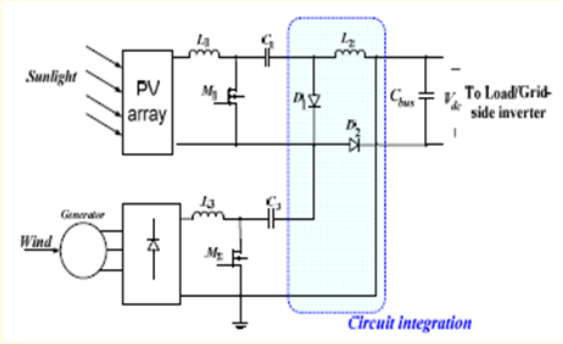

Figure 3: Hybrid Wind/Photovoltaic System Rectifier Stage.

State I (M1 ON, M2 ON):

$$i_{L1} = I_{iPV} + \frac{V_p}{L_1}t \qquad 0 < t < d_1 T_s \qquad \text{-------(16)}$$

$$i_{L2} = I_d + (\frac{V_{c1} + V_{c2}}{L_2})t \qquad 0 < t < d_1 T_s \qquad \text{-----------(17)}$$

$$i_{L3} = I_w + \frac{V_w}{L_3}t \qquad 0 < t < d_1 T_s \qquad \text{----------(18)}$$

State III (M1 OFF, M2 ON):

$$i_{L1} = I_{iPV} + (\frac{V_p - V_{c1}}{L_1})t \qquad d_1 T_s < t < d_2 T_s \qquad \text{------(19)}$$

$$i_{L2} = I_d + \frac{V_{c2}}{L_2}t \qquad d_1 T_s < t < d_2 T_s \qquad \text{------(20)}$$

$$i_{L3} = I_w + \frac{V_w}{L_3}t \qquad d_1 T_s < t < d_2 T_s \qquad \text{------(21)}$$

State IV (M1 OFF, M2 OFF):

$$i_{L1} = I_{iPV} + (\frac{V_p - V_{c1}}{L_1})t \qquad d_2 T_s < t < T_s \qquad \text{------(22)}$$

$$i_{L2} = I_d - \frac{V_d}{L_2}t \qquad d_2 T_s < t < T_s \qquad \text{------(23)}$$

$$i_{L3} = I_w + (\frac{V_w - V_{c2} - V_d}{L_3})t \qquad d_2 T_s < t < T_s \qquad \text{------(24)}$$

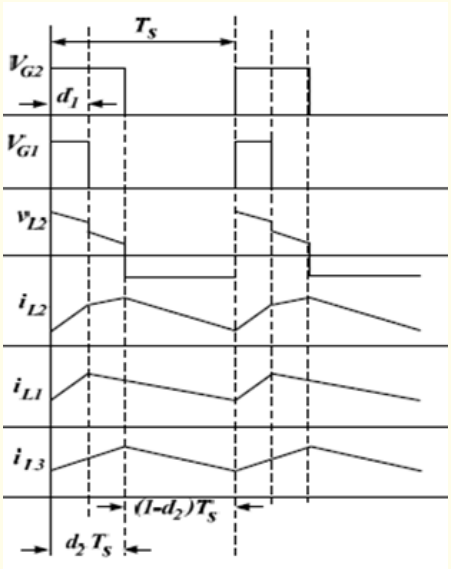

Figure 4: Waveforms for the proposed circuit inductors.

Analysis of proposed circuit

The purpose of this exercise is to derive an expression for the voltage on the DC bus (V_{dc}), as shown in Figure 4, it is necessary to take a look at the voltage-balance of the output inductor, which is denoted by the symbol L_2, with $d_2 > d_1$. The application of volt-balance to L_2, given that there is no overall change in the voltage of L_2, results in the equation (26). It is then possible to derive an expression for the average DC voltage (V_{dc}) and the voltages of the capacitors (v_{c1} and v_{c2}), where v_{c1} and v_{c2} can then be obtained by applying volt-balance to L_1 and L_3 [21-25]. The concluding expression for the relationship between the voltage output by the device on average and both input sources is given by Equation 27. The output voltages of the Cuk and SEPIC converters are simply added together to give V_{dc}, as can be seen. This further demonstrates that V_{dc} can be controlled by either d_1 or d_2 at the same time.

$$(v_{c1} + v_{c2})d_1 T_s + (v_{c2})(d_2 - d_1)T_s + (1 - d_2)(-v_d)T_s = 0 \qquad \text{-------(25)}$$

$$v_{dc} = (\frac{d_1}{1-d_1})v_{c1} + (\frac{d_2}{1-d_2})v_{c2} \qquad \text{-----------(26)}$$

$$v_{dc} = (\frac{d_1}{1-d_1})v_p + (\frac{d_2}{1-d_2})v_w \qquad \text{----------(27)}$$

Also included in this section are the switch's voltage and current characteristics. voltage stress is expressed in terms of equations (28) and (29). On-time MOSFETs exhibit a constant peak current at the end of their on-time period, as shown in Figure 4. Current flowing through the Cuk and SEPIC MOSFETs is a combination of input current and current flowing through the capacitors (C_1 and C_2). The stress at its highest level in M_1 and M_2 can be calculated using the formulas given as per the equations (30) and (32). L_{eq1} and L_{eq2}, provided by equations (31) and (33), represents similarity between Cuk converter and SEPIC converter inductance, respectively. The current that flows from the PV is equivalent to the current that flows through the Cuk converter on average, is given in equation (34). According to the duty cycle of the inductor, the average current can be observed (d_1). Consequently, It is possible to achieve maximum tracking of power points by modifying the number of active shifts for each energy source to the level that is optimal for that source.

$$v_{ds1} = v_{pv}(1 + \frac{d_1}{1-d_1}) \qquad \text{----------(28)}$$

$$v_{ds2} = v_w\left(1+\frac{d_2}{1-d_2}\right) \quad \text{----------(29)}$$

$$i_{ds1,pk} = I_{i,pv} + I_{dc,avg} + \frac{v_{pv} d_1 T_s}{2L_{eq1}} \quad \text{----------(30)}$$

$$L_{eq1} = \frac{L_1 L_2}{L_1 + L_2} \quad \text{----------(31)}$$

$$i_{ds2,pk} = I_{i,w} + I_{dc,avg} + \frac{v_w d_2 T_s}{2L_{eq2}} \quad \text{----------(32)}$$

$$L_{eq2} = \frac{L_3 L_2}{L_3 + L_2} \quad \text{----------(33)}$$

$$I_{i,pv} = \frac{p_0}{v_{dc}} \frac{d_1}{1-d_1} \quad \text{----------(34)}$$

Control of the MPPT on the proposed circuit

Because of the sporadic nature of wind and solar energy, this is a common problem with these systems. A large amount of power can be supplied by wind, but its presence is highly erratic, as it can appear and then disappear at any time. Irradiance of the Sun Changes Throughout the Day Because of the Sun's Changing Intensity and the ever-changing shadows cast by various objects, such as clouds, birds, and trees, ensure that solar energy is always available. Since they have these flaws, renewable energy sources aren't very effective. The effectiveness of the systems can be greatly enhanced by utilising MPPT algorithms (which track the maximum power point). Equation (35) describes the wind's ability to produce mechanical energy in order to describe the power characteristic of a wind turbine.

Pm = 0.5 A Cp (λ, β) v3w ----------(35)

The solar panel system

Solar energy can be put to a wide variety of uses, such as supplying electricity to the main grid, using the electricity to pump water from a well, or even powering a small calculator with the electricity that was generated by solar panels. In order to design a system, one must take into account its purpose and the location where it will be used. This section focuses on the PV system's components, design variations, system sizing, system operation and maintenance.

Another option is to add one or more additional power sources to the system (e.g., a diesel generator or a wind turbine) in order to fulfil certain load requirements. Systems with a hybrid configuration fall under this category.

It is more common for hybrid systems to be used in stand-alone applications rather than grid-connected ones because they allow for a reduction in storage requirements without an increase in load probability. Figure 5 depicts schematic diagrams for the three most common types of systems [26-31].

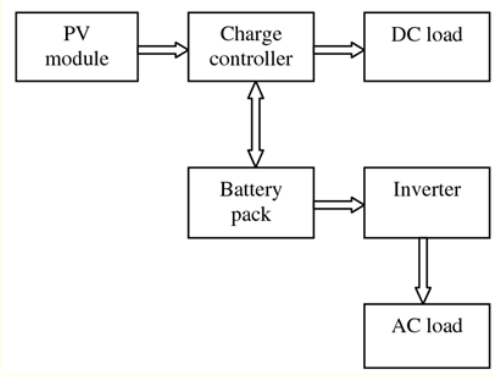

Figure 5: Stand-alone solar power system schematic diagram.

The HCS approach involves changing the system's operating point and then monitoring the results. Depending on whether the output voltage was higher or lower, a positive change in output power will continue to be followed by the control algorithm, so long as the direction of the perturbation is positive. In the event that there is a decrease in output power, the control algorithm will react by reversing the trend of the most recent perturbation step that it carried out in order to compensate. Allowing for a very slight shift in balance of power (within a predetermined area). A system operating point will not change if an algorithm is used that corresponds to the maximum possible power (the point at which the curves' power peaks).

Simulation and Results

It is shown that the proposed multi-input rectifier stage can support both individual and simultaneous operation using PSIM software simulation results in this section. Table 1 contains the design example's specifications.

Output power (W)	1.68 KW
Output voltage	40 V
Switching frequency	18 KHZ

Table 1: Specifications of the rectifier.

Currently, the system is operating with just the PV source (in Cuk converter mode) as a power source because the wind generator has failed. A situation in which the only source of power is a wind turbine (SEPIC converter mode). Finally, figures 6 and 8 is an example of the two sources working together in fusion mode (using Cuk-SEPIC) where the conduction cycle of M_2 is longer (states I, IV, and III of the converter are shown in Figure 3). Both the PV (Cuk) and Wind components of the system are depicted in this figures 5 and 10, which shows the system's MPPT operation.

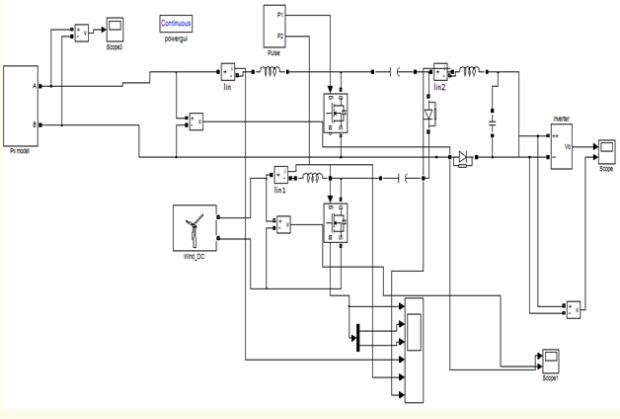

Figure 6: Simulation circuit of a hybrid wind-solar energy system.

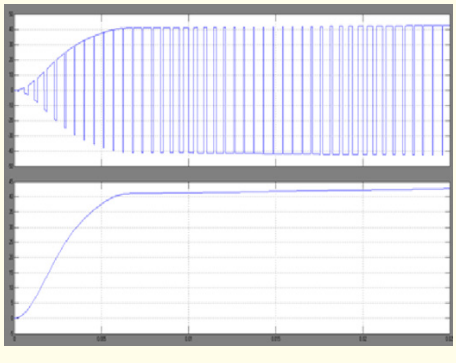

Figure 7: Output waveforms of a hybrid wind-solar energy system.

DC and AC output voltages for CUK-SEPIC are obtained and observed simulation results are shown in the figure 7 to figure 12. Final Cuk-SEPIC mode voltage waveform is shown in figure 12.

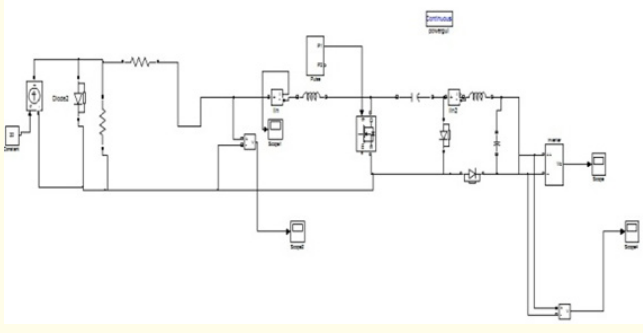

Figure 8: A CUK converter with a photovoltaic cell in simulation.

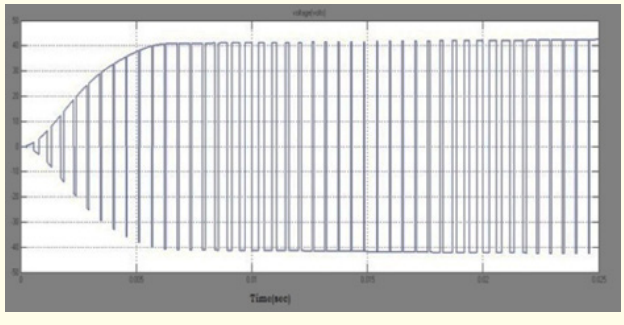

Figure 9: Converter CUK voltage output.

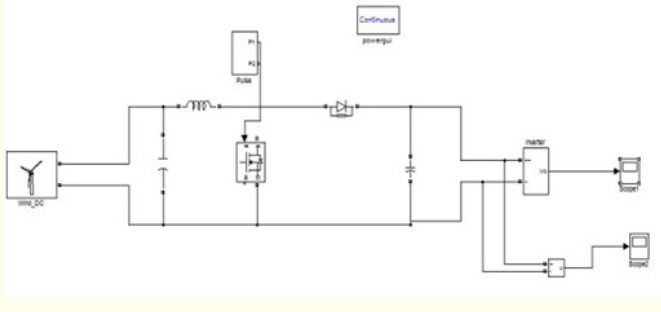

Figure 10: SEPIC converter with wind simulation diagram.

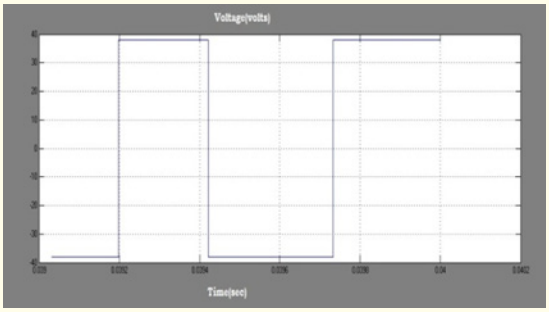

Figure 11: Waveform of the SEPIC AC voltage.

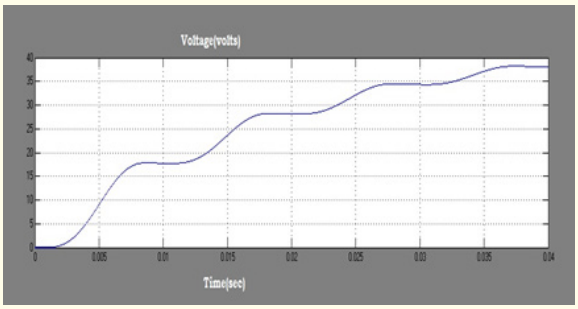

Figure 12: Waveform of the SEPIC DC voltage.

Conclusions

An integrated Cuk-SEPIC converter stage for hybrid wind/solar energy systems is described in this paper. This topology allows for continuous power generation to meet the needs of the load because it allows the load to be supplied by the two sources either separately or jointly. The proposed converter does not require additional input filters to remove harmonics at high frequencies by filtering them out, can handle a wide range of photovoltaic and wind input, has low input current distortion, low conduction losses and an algorithm called Maximum Power Point Tracking that improves its conversion efficiency. To validate the characteristics of the suggested topology, simulation results generated with MATLAB/Simulink have been presented. This system has lower operating costs and finds applications in the aerospace industry, electric vehicles, communication equipment, and rural electrification. In addition, it can generate power in isolated areas, as well as for electric vehicles, energy conversion systems that use either constant or variable speeds, and energy storage systems.

Bibliography

1. Rahman KM., *et al*. "Application of direct-drive wheel motor for fuel cell electric and hybrid electric vehicle propulsion system". *IEEE Transactions on Industry Applications* 42.5 (2006): 1185-1192.

2. Hinkkanen M and Luomi J. "Induction motor drives equipped with diode rectifier and small DC-link capacitance". *IEEE Transactions on Industrial Electronics* 55.1 (2008): 312-320.

3. Rivetta C H., *et al*. "Analysis and control of a buck DC-DC converter operating with constant power load in sea and undersea vehicles". *IEEE Transactions on Industry Applications* 42.2 (2006): 559-572.

4. Kim SK., *et al*. "Dynamic modeling and control of a grid-connected hybrid generation system with versatile power transfer". *IEEE Transactions on Industrial Electronics* 55.4 (2008): 1677-1688.

5. Rodriguez J., *et al*. "Multilevel inverters: a survey of topologies, controls, and applications". *IEEE Transactions on Industrial Electronics* 49.4 (2002): 724-738.

6. Ahmed NA., *et al*. "Power fluctuations suppression of standalone hybrid generation combining solar photovoltaic/wind turbine and fuel cell systems". *Energy Conversion and Management* 49.10 (2008): 2711-2719.

7. Jain S and Agarwal V. "An integrated hybrid power supply for distributed generation applications fed by nonconventional energy sources". *IEEE Transactions on Energy Conversion* 23.2 (2008): 622-631.

8. Tolbert L M., *et al*. "Multilevel PWM methods at low modulation indices". *IEEE Transactions on Industrial Electronics* 15.4 (2000): 719-725.

9. Chen YM., *et al*. "Multi-input inverter for grid-connected hybrid PV/wind power system". *IEEE Transactions on Industrial Electronics* 22.3 (2007): 1070-1077.

10. Ganesh P., *et al*. "A renewable hybrid wind solar energy system fed single phase multilevel inverter". *International Journal of Engineering Research and Technology (IJERT)* 3.1 (2014).

11. Challa D and Inguva R. "An inverter fed with combined wind-solar energy system using CUK-SEPIC converter.". *International Journal of Engineering Research and Technology* 9 (2012): 1-8.

12. Shen M and Peng FZ. "Operation modes and characteristics of the Z-source inverter with small inductance or low power factor". *IEEE Transactions on Industrial Electronics* 55.1 (2008): 89-96.

13. Al-Buraiki AS., *et al*. "Hydrogen production via using excess electric energy of an off-grid hybrid solar/wind system based on a novel performance indicator". *Energy Conversion and Management,* 254 (2022): 115270.

14. Bakhtvar M., *et al*. "A vision of flexible dispatchable hybrid solar-wind-energy storage power plant". *IET Renewable Power Generation* 15.13 (2021): 2983-2996.

15. Bakir H and Kulaksiz A A. "Modelling and voltage control of the solar-wind hybrid micro-grid with optimized STATCOM using GA and BFA". *Engineering Science and Technology, an International Journal* 23.3 (2020): 576-584.

16. Cao Y., *et al*. "Design, dynamic simulation, and optimal size selection of a hybrid solar/wind and battery-based system for off-grid energy supply". *Renewable Energy* 187 (2022): 1082-1099.

17. Diab AAZ., *et al*. "Optimal sizing of hybrid solar/wind/hydroelectric pumped storage energy system in Egypt based on different meta-heuristic techniques". *Environmental Science and Pollution Research* 27.26 (2020): 32318-32340.

18. Ekren O., *et al*. "Sizing of a solar-wind hybrid electric vehicle charging station by using HOMER software". *Journal of Cleaner Production* 279 (2021): 123615.

19. Eryilmaz S., *et al*. "Reliability based modeling of hybrid solar/wind power system for long term performance assessment". *Reliability Engineering and System Safety* 209 (2021): 107478.

20. Guangqian D., *et al*. "A hybrid algorithm based optimization on modeling of grid independent biodiesel-based hybrid solar/wind systems". *Renewable Energy* 122 (2018): 551-560.

21. Javed M S., *et al*. "Techno-economic assessment of a stand-alone hybrid solar-wind-battery system for a remote island using genetic algorithm". *Energy* 176 (2019): 704-717.

22. Kamel S., *et al*. "Sizing and evaluation analysis of hybrid solar-wind distributed generations in real distribution network considering the uncertainty". 2019 International Conference on Computer, Control, Electrical, and Electronics Engineering (ICCCEEE) (2019).

23. Masih A and Verma H. "Optimization and reliability evaluation of hybrid solar-wind energy systems for remote areas". *International Journal of Renewable Energy Research (IJRER)* 10.4 (2020): 1697-1706.

24. Mehrjerdi H. "Modeling and optimization of an island water-energy nexus powered by a hybrid solar-wind renewable system". *Energy* 197 (2020): 117217.

25. Peng W., *et al*. "Optimization of a hybrid system for solar-wind-based water desalination by reverse osmosis: comparison of approaches". *Desalination* 442 (2018): 16-31.

26. Sen A., *et al*. "A comparative analysis between two DPFC models in a grid connected Hybrid Solar-Wind Generation system". 2020 IEEE International Conference on Power Electronics, Smart Grid and Renewable Energy (PESGRE2020) (2020).

27. Shivaie M., *et al*. "A reliability-constrained cost-effective model for optimal sizing of an autonomous hybrid solar/wind/diesel/battery energy system by a modified discrete bat search algorithm". *Solar Energy* 189 (2019): 344-356.

28. Tahiri F., *et al*. "Optimal management energy system and control strategies for isolated hybrid solar-wind-battery-diesel power system". *Emerging Science Journal* 5.2 (2021): 111-124.

29. Xu B., *et al*. "Modeling a pumped storage hydropower integrated to a hybrid power system with solar-wind power and its stability analysis". *Applied Energy* 248 (2019): 446-462.

30. Yang J., *et al*. "Optimal capacity and operation strategy of a solar-wind hybrid renewable energy system". *Energy Conversion and Management* 244 (2021): 114519.

31. Zhang W., *et al*. "Sizing a stand-alone solar-wind-hydrogen energy system using weather forecasting and a hybrid search optimization algorithm". *Energy Conversion and Management* 180 (2019): 609-621.